UNITED STATES

DEPARTMENT OF THE INTERIOR

GEOLOGICAL SURVEY

DO P- AND S-WAVE CORNER FREQUENCIES MEASURE DIFFERENT SOURCE PARAMETERS?

By

W. H. Bakun, C. G. Bufe and R. M. Stewart
345 Middlefield Road
Menlo Park, CA 94025

Open File Report 80-602

Do P- and S-Wave Corner Frequencies Measure Different Source Parameters?

W. H. Bakun, C. G. Bufe and R. M. Stewart

U.S. Geological Survey

345 Middlefield Road

Menlo Park, CA 94025

There is a systematic difference in the magnitude dependence of P- and SH-wave corner frequencies (Bakun et al., 1976) that can be explained using simple dislocation models if the usual assumption of similarity (see Aki, 1967) is relaxed, e.g., if rupture-propagation velocity increases with source size from 0.6β for $M \simeq 2$ to 0.9β for $M \simeq 4$. Relaxation of similarity has profound implications for the interpretation of body-wave data in terms of earthquake source parameters. In relating their scaling model for 1965 Rat Island earthquakes to shocks on the San Andreas fault in central California, Frasier and North (1978) ascribed systematic differences in the magnitude dependence of the corner frequencies they inferred from the data of O'Neill and Healy (1973) and the corner frequencies of Johnson and McEvilly (1974) to the fact that O'Neill and Healy's were measured in the time domain and Johnson and McEvilly's in the frequency domain. A likelier explanation is that the difference is a function of P-wave relative to Love-wave measurements, since O'Neill and Healy's P-wave data are consistent with the P-wave corner frequencies of Bakun et al. (1976).

We here consider the source-parameter data of O'Neill and Healy (1973), Johnson and McEvilly (1974), and Bakun et al. (1976) for earthquakes located near the San Andreas fault zone in central California (see Figure 1). All of the shocks studied by O'Neill and Healy and by Bakun et al. and four of the thirteen events studied by Johnson and McEvilly are located within a 10-km-long segment of the fault zone. The relation of corner frequency and magnitude is shown in Figure 2. Solid circles are the corner frequencies calculated from O'Neill and Healy's source dimensions by Frasier and North (1978). Open circles represent Johnson and McEvilly's data. The P- and S-wave corner frequencies of Bakun et al. are shown as solid and open diamonds respectively; For our data we have disregarded uncertain corner frequencies (marked by an asterisk in Table 2 of Bakun et al.).

O'Neill and Healy's (1973) measurements were for P waves in the time domain. Johnson and McEvilly utilized a 41-second time window to obtain source spectra from horizontal-component seismograms; their corner frequencies probably are primarily a measure of the Love wave (see Figure 4 of their paper). The P- and SH- corner frequencies of Bakun et al. were measured in the frequency domain. Note that the P-wave corner frequencies inferred by Frasier and North (1978) from O'Neill and Healy's measurements of the duration of the first half-cycle of motion are in excellent agreement with the P-wave corner frequencies of Bakun et al.. P-wave corner frequencies decrease monotonically with magnitude from 20 Hz for M_L 1.0 to 2 Hz for M_L 4.0, while the Love-wave corner frequencies of Johnson and McEvilly and the SH-wave corner frequencies of Bakun et al. show only a weak dependence of corner frequency on magnitude. The decade difference between the whole-record Love-wave corner

frequencies ($\simeq$ 1 to 2 Hz) of Johnson and McEvilly and the SH-wave corner frequencies ($\simeq$ 10 to 20 Hz) of Bakun et al. must be bound up in the details of the generation and propagation of the shear phases constituting the Love wave. It is well known that whole-record Love-wave spectra depend on both structure and focal depth as shown, for example, in the work of Tsai and Aki (1970) and Heaton and Helmberger (1977). Since focal depths of shocks considered by Johnson and McEvilly (1974) range from 3 to 12 km, their 1 to 2 Hz whole-record Love-wave corner frequencies probably are a measure of structure in the upper crust. Bakun et al. (1978) have shown that whereas body-wave spectra of microearthquakes on this section of the fault reflect source parameters, the character of the seismic coda is controlled by local crustal structure.

Even for simple dislocation models, predicted corner frequencies can be affected by a number of source-model parameters — velocities and directions of rupture propagation, the P-wave and S-wave velocities, the orientation, size, and shape of the slipped surface and the location of the hypocenter within that surface, the rise time and orientation of the slip vector, and the azimuth and takeoff angle to the recording site. Given the lack of constraints, a wide range of corner-frequency relations is possible. To reduce the number of independent source parameters, Aki (1967) introduced the concept of similarity; i.e., large and small earthquakes are similar phenomena. If earthquakes are geometrically and physically similar, then rupture velocity is constant and all source parameters having dimensions of time or distance are proportional to source length L (Aki, 1967).

Corner frequencies expected at station BIC for three of the shocks studied by Bakun et al. (1976) have been calculated using Savage's (1972) Haskell fault model (see Table 1), which assumes simultaneous slip across the fault width and bilateral rupture along the fault length L at constant rupture velocity v. Slip at every point on the fault is assumed to be the same. We consider rupture-propagation velocity equal to β , 0.9β , 0.8β , and 0.6β and two azimuths corresponding to an homogeneous crust (Θ = 12.5° for a great circle path) and to velocity increasing with distance from the fault zone (Θ = 33°). Whereas there is strong evidence for lateral refraction of P waves (see Bakun et al., 1976), S waves are apparently not so severely refracted (W. H. Bakun, C. G. Bufe, and R. M. Stewart, unpublished data; A. Levander, unpublished data). For fixed geometry and constant rupture propagation velocity v, the ratio of the S- to P-wave corner frequencies, f_o^S/f_o^P, is independent of source length (Table 1), contrary to the evidence of the data in Figure 2. For each of the three events in Table 1, certain source lengths, shown italicized, have f_o^S/f_o^P comparable to that predicted by the model. V increasing from 2.1 km/sec (0.6β) for M = 1.8 to 3.1 km/sec (0.9β) = Rayleigh velocity for M = 4.1 satisfies the observed dependence of f_o^S/f_o^P on magnitude. Note that the P-wave data of Figure 2 obtained for several source-to-receiver azimuths (stations BIC, CNR, SJG, and JHC in Figure 1) show little scatter, consistent with limited azimuthal variation in corner frequency for subsonic rupture propagation velocities (see Figure 1 of Savage, 1972). Computed source lengths range from 70 m for M = 1.8 to 0.52 km for M = 4.1. Corresponding rupture propagation times, i.e., L/v, are 0.033 and 0.17 sec. These data suggest that if big shocks grow from small ones, then v increases as the source grows. Specifically, the average rupture-propagation

velocity for the initial 1/30 sec (70 m of source length) is 0.6 β and approaches the Rayleigh velocity after 0.2 sec when source length equals 1/2 km. Analysis of the growth of fracture suggests that v should increase fairly rapidly to a critical value lying between the Rayleigh (0.9β) and shear velocity β (Kostrov, 1970). It should be noted that an increase in rupture-propagation velocity with source size is only one of several relaxations of the similarity assumption that will satisfy these corner-frequency data. For example, a specific systematic variation in the ellipticity of the source region with magnitude could also result in the systematic difference in the magnitude dependence of P- and S-wave corner frequencies shown in Figure 2.

P- and S-wave corner frequencies are generally interpreted in terms of the source dimension of the earthquake (see e.g., Brune, 1970; Hanks and Wyss, 1972; Savage, 1972). If similarity cannot be assumed, then it is not clear which, and how many, of the several source paramenters scale with source length. That is, corner frequencies in general are related through a nonlinear function to several model parameters, and reliable inference of earthquake parameters from seismic data requires detailed knowledge of that function. Specifically, corner frequencies may not be simply related to source dimension;if they are not, stress drop cannot be easily inferred from corner frequency observations. It should be emphasized that failure of the similarity assumption has been demonstrated only for shocks located on a 10-km-long section of the San Andreas fault in central California. The only other data set recorded with sufficient dynamic range to detect a systematic dependence of f_o^s/f_o^p with magnitude are the aftershocks of the 1971 San Fernando, California, earthquake (Tucker and Brune, 1973).

REFERENCES

Aki, K. (1967). Scaling law of seismic spectrum, J. Geophys. Res., 72, 1217-1231.

Bakun, W. H., R. M. Stewart, and C. G. Bufe, (1978). Directivity in the high-frequency radiation of small earthquakes, Bull. Seism. Soc. Am. 68, 1253-1263.

Bakun, W. H., C. G. Bufe, and R. M. Stewart (1976). Body-wave spectra of central California earthquakes, Bull. Seism. Soc. Am., 66, 363-384.

Brune, J. N. (1970). Tectonic stress and the spectra of seismic shear waves from earthquakes, J. Geophys. Res., 75, 4997-5009.

Frasier, C. W., and R. G. North (1978). Evidence for ω-cube scaling from amplitudes and periods of the Rat Island sequence (1965), Bull. Seism. Soc. Am., 68, 265-282.

Hanks, T. C., and M. Wyss (1972). The use of body-wave spectra in the determination of seismic-source parameters, Bull. Seism. Soc. Am., 62, 561-589.

Heaton, T. H., and D. V. Helmberger (1977). A study of the strong ground motion of the Borrego Mountain, California, earthquake, Bull. Seism. Soc. Am., 67, 315-330.

Johnson, L. R. and T. V. McEvilly (1974). Near-field observations and source parameters of central California earthquakes, Bull. Seism. Soc. Am., 64, 1855-1886.

Kostrov, B. V. (1970). The theory of the focus for tectonic earthquakes, Izv. Acad. Sci. USSR Phys. Solid Earth, English transl., no. 4, 258-267.

O'Neill, M. E. and J. H. Healy (1973). Determination of source parameters of small earthquakes from P-wave rise time, Bull. Seism. Soc. Am., 63, 599-614.

Savage, J. C. (1972). Relation of corner frequency to fault dimensions, J. Geophys. Res., 77, 3788-3795.

Tsai, Y. B., and K. Aki (1970). Precise focal depth determination from amplitude spectra of surface waves, J. Geophys. Res., 75, 5729-5743.

Tucker, B. E., and J. N. Brune (1973). Seismograms, S-wave spectra , and source parameters for aftershocks of the February 8, 1972 San Fernando earthquake, San Fernando, California, Earthquake of February 9, 1971, Vol. III, 69-121, published by the U.S. Department of Commerce, Washington, D. C., 69-122.

Figure Captions

Figure 1. Location of seismograph stations and epicenters with respect to the trace of the San Andreas fault zone in central California. Stations used by Johnson and McEvilly: San Andreas Geophysical Observatory East and Central (SAGO E and SAGO C); by O'Neill and Healy: Cienega Road (CNR), San Juan Grade (SJG), and Johnson Canyon (JHC); and by Bakun et al.: Bickmore Canyon (BIC) are shown as triangles. Hatching represents the 10-km-long segment of the fault that encompasses shocks for which data are shown in Figure 2.

Figure 2. The relation of magnitude and corner frequency (adapted from Figure 13 of Frasier and North, 1978).

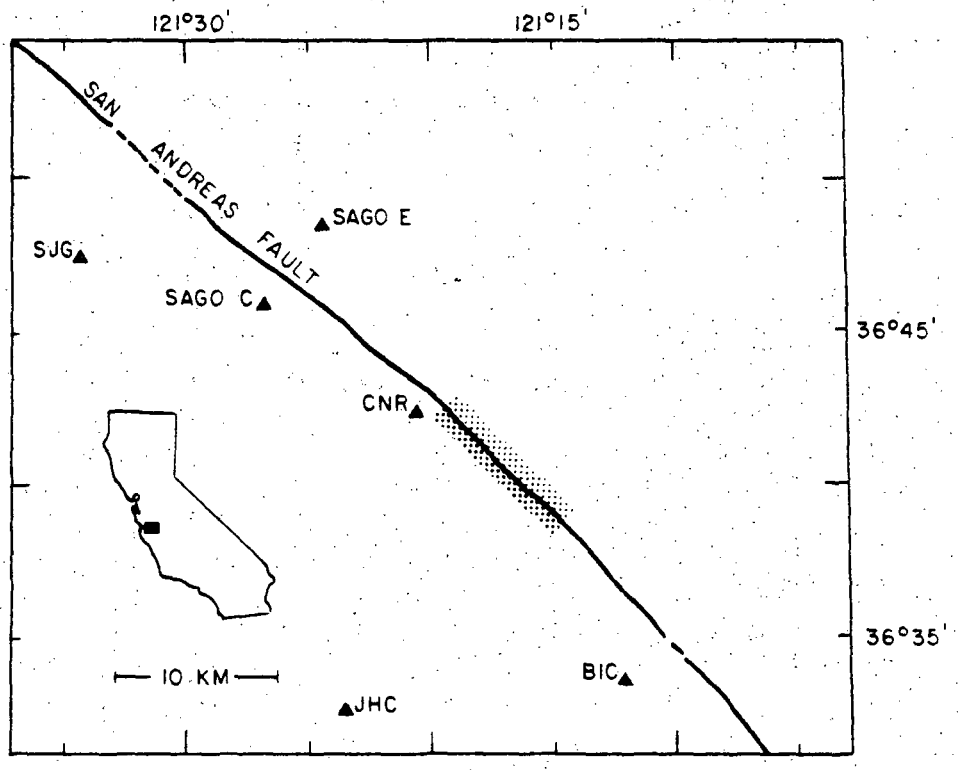
121°30'
121°15'
SAN ANDREAS FAULT
SAGO E
SJG
SAGO C
CNR
36°45'
36°35'
10 KM
BIC
JHC

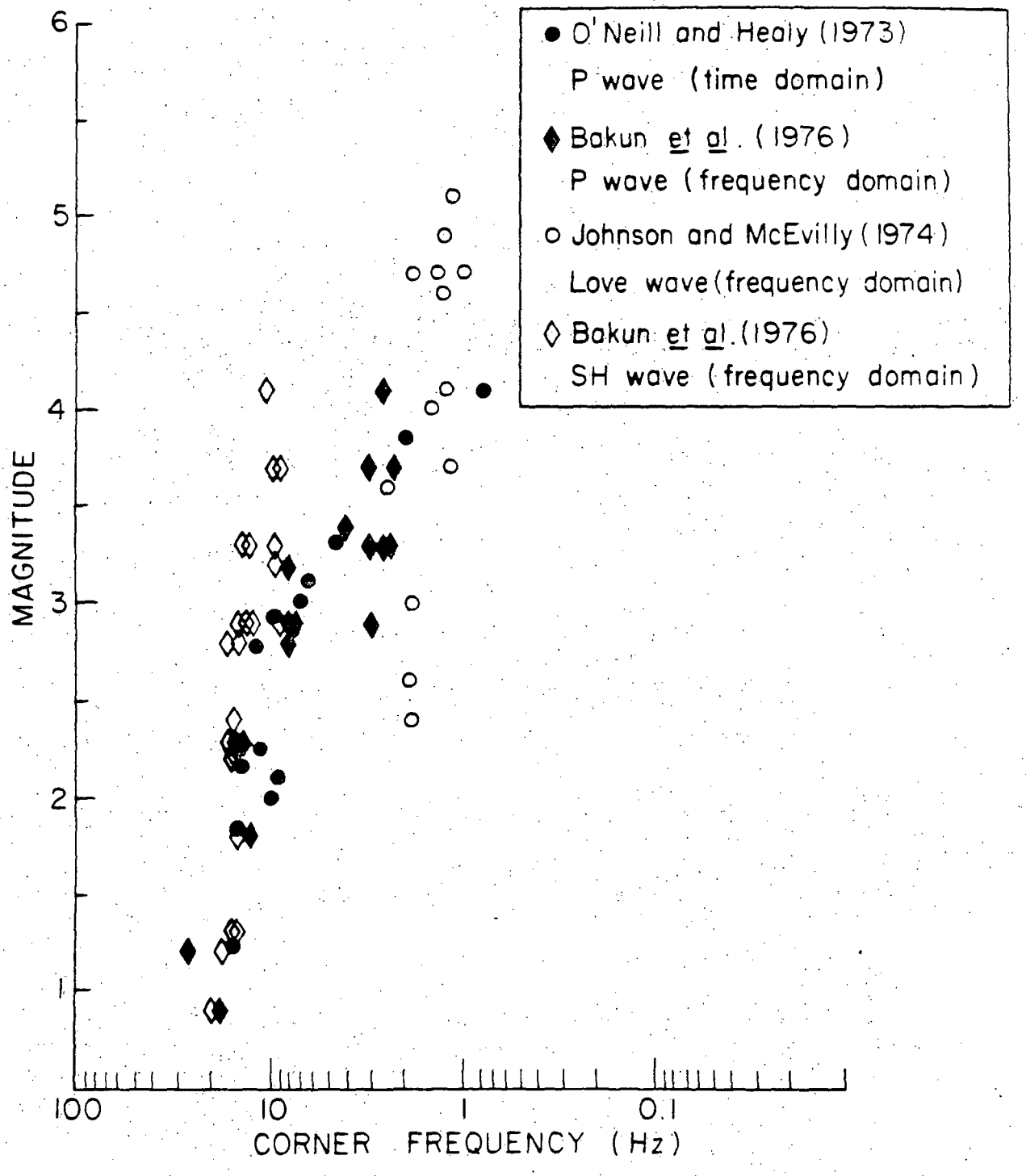
● O'Neill and Healy (1973)
P wave (time domain)
♦ Bakun et al. (1976)
P wave (frequency domain)
○ Johnson and McEvilly (1974)
Love wave (frequency domain)
◇ Bakun et al. (1976)
SH wave (frequency domain)
MAGNITUDE
6
5
4
3
2
1
100
10
1
0.1
CORNER FREQUENCY (Hz)

Figure...

TABLE 1. SOURCE PARAMETERS

v	θ	$f_o^P \cdot L$*	$f_o^S \cdot L$*	f_o^S/f_o^P	M_L 4.1† L from f_o^P	M_L 4.1† L from f_o^S	M_L 2.9†† L from f_o^P	M_L 2.9†† L from f_o^S	M_L 1.8††† L from f_o^P	M_L 1.8††† L from f_o^S
3.5 km/sec	33°	1.62	8.30	5.12	0.65 km	0.83 km	0.27 km	0.59 km	0.14 km	0.59 km
	12.5°	1.89	31.1	16.5	0.76	3.1	0.32	2.22	0.16	2.22
				19.20§						
3.1	33°	1.32	2.74	2.08	*0.53*§	*0.27*	0.22	0.20	0.11	0.20
	12.5°	1.48	5.19	3.51	*0.59*	*0.52*§	0.25	0.37	0.12	0.37
				3.93§						
2.8	33°	1.33	1.94	1.46	0.53	0.19	*0.22*§	*0.14*	0.11	0.14
	12.5°	1.23	2.89	2.35	0.49	0.29	*0.21*	*0.21*§	0.10	0.21
				2.17§						
2.1	33°	0.76	1.00	1.32	0.30	0.10	0.13	0.071	*0.063*§	*0.071*
	12.5°	0.80	1.18	1.48	0.32	0.12	0.13	0.084	*0.067*	*0.084*§
				1.55§						

* Calculated using eqn. 13 of Savage (1972): $\omega^c = 2\pi f_o^c = (\frac{2c}{L})[(\frac{c}{v})^2 + \cos^2\theta]^{\frac{1}{2}}/[(c/v)^2 - \cos^2\theta]$, where c = phase velocity (α or β), f_o^c = corner frequency (Hz), L = fault length, v = rupture propagation velocity, θ = angle between seismic ray leaving the source and the rupture propagation direction.

§ θ = 12.5° for the great circle azimuth and 33° is more appropriate for lateral refraction. We prefer θ = 12.5° for S and θ = 33° for P.

† Event #1 of Bakun et al. (1976). f_o^P = 2.5 Hz, f_o^S = 10 Hz, f_o^S/f_o^P = 4

†† Event #3 of Bakun et al. (1976). f_o^P = 6 Hz, f_o^S = 14 Hz, f_o^S/f_o^P = 2.3

††† Event #18 of Bakun et al. (1976). f_o^P = 12 Hz, f_o^S = 14 H, f_o^S/f_o^P = 1.2

L shown in italics are source lengths for which observed and theoretical f_o^S/f_o^P are comparable.